

## LOW ENERGY ION SCATTERING STUDY OF OXYGEN ADSORPTION ON A Cu{100} SINGLE CRYSTAL SURFACE

### Part I: Surface characteristics

Th.M. HUPKENS \*

*Fysisch Laboratorium der Rijksuniversiteit Utrecht, Princetonplein 5, 3584 CC Utrecht, The Netherlands*

Received 21 December 1984 and in revised form 22 February 1985

The surface characteristics of the oxygen-covered Cu{100} surface have been studied using Low Energy Ion Scattering. The results indicate that already at the second adsorption stage (LEED:  $(\sqrt{2} \times \sqrt{2})R45^\circ - O$  structure) two essentially different oxygen positions are involved. There are some indications that in the third adsorption stage (LEED:  $(\sqrt{2} \times 2\sqrt{2})R45^\circ - O$  structure) oxygen incorporation into the selvedge takes place. The structure in the azimuthal distributions of  $O^-$  recoil ions is in accordance with two essentially different oxygen positions, possibly at the positions as proposed by Onuferko and Woodruff: in this model oxygen is initially adsorbed into 2-fold bridge sites 1.4 Å above the surface and subsequently incorporated into 4-fold sites in the first copper surface layer.

After oxygen exposures in the second stage a copper surface that is not reconstructed is observed.

### 1. Introduction

Despite many efforts during the last two decades, the position of adsorbed oxygen atoms on a Cu{100} surface has still not been unambiguously determined [1–17]. With LEED the following sequence of patterns is observed (see also table 1):

- *stage A*: for low exposures ( $\sim 0.08 \text{ Pa} \cdot \text{s}$ ) a so-called “four spot” pattern, corresponding to an “oblique net” with vectors along the [051] and the [017] directions in four different orientations [1–3,9]. This structure was not observed by some authors [5,13]. In all cases an increasing background was observed in this adsorption stage, indicative of disordered adsorption.
- *stage B*: for higher exposures ( $\sim 0.1 \text{ Pa} \cdot \text{s}$ ) the four spot pattern changes into the  $(\sqrt{2} \times \sqrt{2})R45^\circ - O$  structure.
- *stage C*: at room temperature this structure changes gradually into the  $(\sqrt{2} \times 2\sqrt{2})R45^\circ - O$  structure for somewhat higher exposures ( $\sim 0.3 \text{ Pa} \cdot \text{s}$ ). Instead of the latter structures different LEED patterns were observed in some studies (see table 1)

It is now generally assumed that the  $(\sqrt{2} \times \sqrt{2})R45^\circ - O$  structure corresponds to 0.5 monolayers; some authors assume that the fully developed  $(\sqrt{2} \times 2\sqrt{2})R45^\circ - O$  structure corresponds to 0.75 monolayers [13b]. From work function measurements ( $\delta\phi$ )

\* Present address: Kamerlingh Onnes Laboratorium der Rijksuniversiteit Leiden, Nieuwsteeg 18, 2311 SB Leiden, The Netherlands.

and Auger-spectroscopy (AES) it is deduced that oxygen incorporation in the selvedge occurs at stage C [7,9,13].

In the past a number of possible positions have been put forward for the adsorbed oxygen atoms (see table 1). From this list of proposed sites it becomes clear that the problem of finding the position(s) of adsorbed oxygen atoms is far from being solved.

### 2. Experimental

The apparatus consists basically of a stainless steel ultra high vacuum chamber, pumped by a 500 l/s turbomolecular pump via an  $LN_2$  trap, which also contained a Ti-sublimation unit (base pressure  $2 \times 10^{-8}$  Pa). The ion source was differentially pumped to a pressure of about  $2 \times 10^{-6}$  Pa. The electron-impact source and lens system are described elsewhere [25]. An electrostatic double flat-plate energy analyser, described elsewhere [19,26,27], was used. This analyser could be rotated around the surface in the plane defined by the incoming beam direction and the surface normal. The angular resolution in this plane was  $4^\circ$ . The energy resolution was 4%.

The crystal was mounted in a target manipulator, which has been described elsewhere [23]. With this manipulator the polar angle of incidence  $\psi$  and the azimuthal angle  $\phi$  could be varied between  $0^\circ$  and about  $370^\circ$  within an accuracy of  $0.2^\circ$ . Both rotations were computer-controlled, which made it possible to measure automatically a complete  $\phi$ - $\psi$  picture (“photo-

Table 1  
Proposed surface characteristics for Cu{100}+O<sub>ad</sub>

Ref.	Technique	Proposed adsorption sites, reconstruction, situation in the surface region	Exposure (Pa · s)
<i>Stage A.</i> “Four-spot pattern” (oblique structure): it is assumed that no reconstruction takes place during this stage			
[1]	LEED	2-fold bridge + 4-fold sites: $\theta_{\text{sat}} = 0.5$	0.01–0.08
[2]	LEED spot size	oxygen in domains of about 100 Å diameter	0.01
[3]	among others LEED	no structure was found that could explain all features of the observed LEED pattern	0.01
[9]		“four-spot pattern” is explained by phase/antiphase splitting of some spots of the (subsequent) $(\sqrt{2} \times \sqrt{2})R45^\circ - O$ structure	
<i>Stage B.</i> Cu{100} $(\sqrt{2} \times \sqrt{2})R45^\circ - O$ structure (in literature also referred to as $p(1 \times 1)$ or $c(2 \times 2)$ structure): $\theta_{\text{sat}} = 0.5$			
[3]	LEED	unstable structure (transition between four-spot and $(\sqrt{2} \times \sqrt{2})R45^\circ - O$ structure	0.01–0.4
[5,6]	LEED intensity analysis	alternate oxygen and copper atoms in the first surface layer; expansion (5–10)%	0.08
[7]	ARPES <sup>a)</sup>	no reconstruction	< 0.3
[9]	LEED	4-fold sites; no reconstruction	0.1
[11]	angle-resolved SIMS	4-fold sites 1.2–1.5 Å above the first copper surface layer	0.16
[12]	angle-resolved XPS	4-fold sites <i>in</i> the first surface layer	0.16
[14]	LEED intensity analysis	oxygen adsorption <i>above</i> the copper surface	> 0.03
[15]	ARPES <sup>a)</sup>	4-fold sites	0.13
[16,17]	LEED, LEIS	initial adsorption into 2-fold bridge sites 1.4 Å above the surface and subsequent incorporation into 4-fold sites in the first copper surface layer (mixed $(\sqrt{2} \times \sqrt{2})R45^\circ - O$ and $(\sqrt{2} \times 2\sqrt{2})R45^\circ - O$ structure)	0.13
[30]	LEED intensity analysis	4-fold sites, 1.8 Å above the copper surface	
<i>Stage C.</i> Cu{100} $(\sqrt{2} \times 2\sqrt{2})R45^\circ - O$ structure (in literature also referred to as $(2 \times 4) - 45^\circ$ or $(2 \times 1)$ structure)			
[1,2]	LEED, $\delta\phi$	penetration of oxygen into the crystal and rearrangement of the copper atoms of at least the top two atomic layers	> 0.24 0.08
[3]	LEED	two domain orientations	0.4–0.8
[5]	LEED	a $(2 \times 2)$ structure was found, probably due to a different target preparation	0.8
[7,9]	ARPES <sup>a)</sup> , LEED.	incorporation of oxygen and rearrangement of copper atoms	> 0.3
[8]	angle-resolved AES	no reconstruction	0.08 + annealing
[9]	LEED, $\delta\phi$	oxygen incorporation into the selvedge	0.5
[16,17]		see stage B	

<sup>a)</sup> ARPES = angle resolved photo electron spectroscopy.

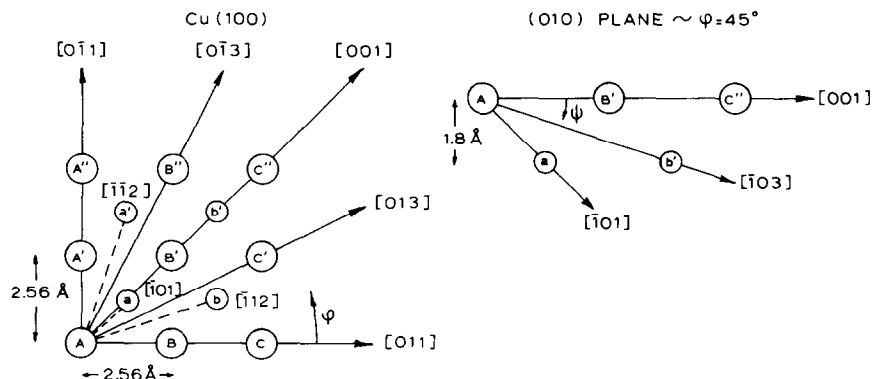


Fig. 1. Diagram of the first and second surface layer of a Cu(100) surface.

gram" [21,22]). We define the azimuthal direction of incidence with respect to the [011] azimuthal direction (see fig. 1). The crystals were heated by placing an infrared heater in front of the crystal. The temperature was measured at the back of the crystal by a platinum resistance thermometer.

### 3. Target preparation

The Cu(100) single crystals were supplied by the late Dr. B. Knook (Kamerlingh Onnes Laboratory, Leiden). After the orientation of the 5N single crystal rod had been checked by Laue X-ray back-reflection, disc shaped samples with a diameter of 3 mm were spark-cut. The crystals were mechanically and electro-lap polished just before they were mounted in the target manipulator. The surface was further cleaned in vacuum by cycles of annealing (800 K) and sputtering (4 keV Ne<sup>+</sup> ions at a small incidence angle) until polar distributions of backscattered ions showed no surface irregularities, except for possible steps that are present due to a slight misorientation of the crystal surface (see ref. [24]). The sample that was used was cut with an approximate deviation of the {100} plane of 0.7°.

### 4. The "visibility" of adsorbed oxygen atoms

In energy spectra that were recorded for the incidence direction along the surface [011] direction ( $\phi = 0^\circ$ ) at specular reflection with  $\psi = 22^\circ$  three oxygen-related signals are clearly visible (see fig. 2). Apparently the oxygen atoms are not shadowed in this direction. If the azimuthal direction is changed to the [100] direction ( $\phi = 45^\circ$ ), the O<sup>-</sup> peak is less pronounced than it was at  $\phi = 0^\circ$  but clearly visible (see fig. 3). In the spectrum for positive ions a broad peak is observed, in which the O<sup>+</sup> recoil peak and the Ne<sup>+</sup> | O reflection peak cannot be distinguished. It is worth noting that a similar broad peak was observed for the O/Cu(110) surface, if comparable directions of incidence and detection were used. (This peak causes the sharp black spot in the O<sup>+</sup> recoil photogram of the oxygen-covered Cu(110) surface in refs. [21,22].) The nature of this broad peak is not yet completely understood, but certainly multiple collisions are involved. It is found that the transition from the two well-separated peaks for  $\phi = 0^\circ$  to the broad maximum for  $\phi = 45^\circ$  takes place gradually via a shift of the O<sup>+</sup> recoil peak to lower energies and a shift of the Ne<sup>+</sup> | O<sub>ad</sub> reflection peak to higher energies. Therefore it is not meaningful to measure azimuthal distributions if the selected energy is fixed at either the O<sup>+</sup> recoil peak or the Ne<sup>+</sup> | O<sub>ad</sub> reflection peak.

The O<sup>-</sup> peak on the other hand showed only a small shift towards higher energies for  $\phi = 45^\circ$  or for small

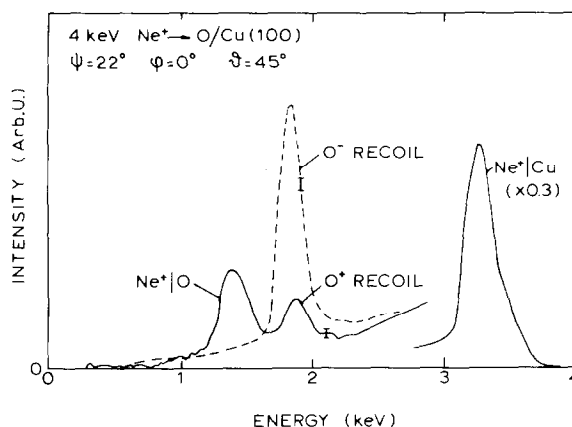


Fig. 2. Energy spectra for an oxygen-covered Cu(100) surface at  $\phi = 0^\circ$  ( $-[011]$ ).

angles of incidence. The maximum shift appeared to be so small that all azimuthal distributions could be measured with a fixed detection energy. We estimate that the error in the intensities, measured in this way, is at most 10%.

A photogram of the O<sup>-</sup> recoil intensity for an oxygen-covered Cu(100) surface (stage B) is shown in fig. 4. A considerable O<sup>-</sup> intensity is measured for all directions of incidence, including the directions where shadowing or blocking occurs (see also fig. 5). These shadowing zones are white in the photograms, because of the limited number of grey-shades available. It appears difficult to interpret azimuthal distributions and photograms for {100} surfaces:

- the range of azimuthal incidence directions that contains all information is only  $45^\circ$ .
- If a superstructure with a lower symmetry is formed which is present at the surface in domains with a different azimuthal orientation, then shadowing of

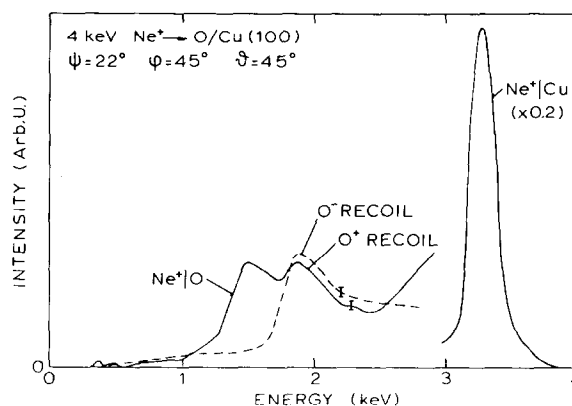


Fig. 3. Energy spectrum for an oxygen-covered Cu(100) surface at  $\phi = 45^\circ$  ( $-[001]$ ).

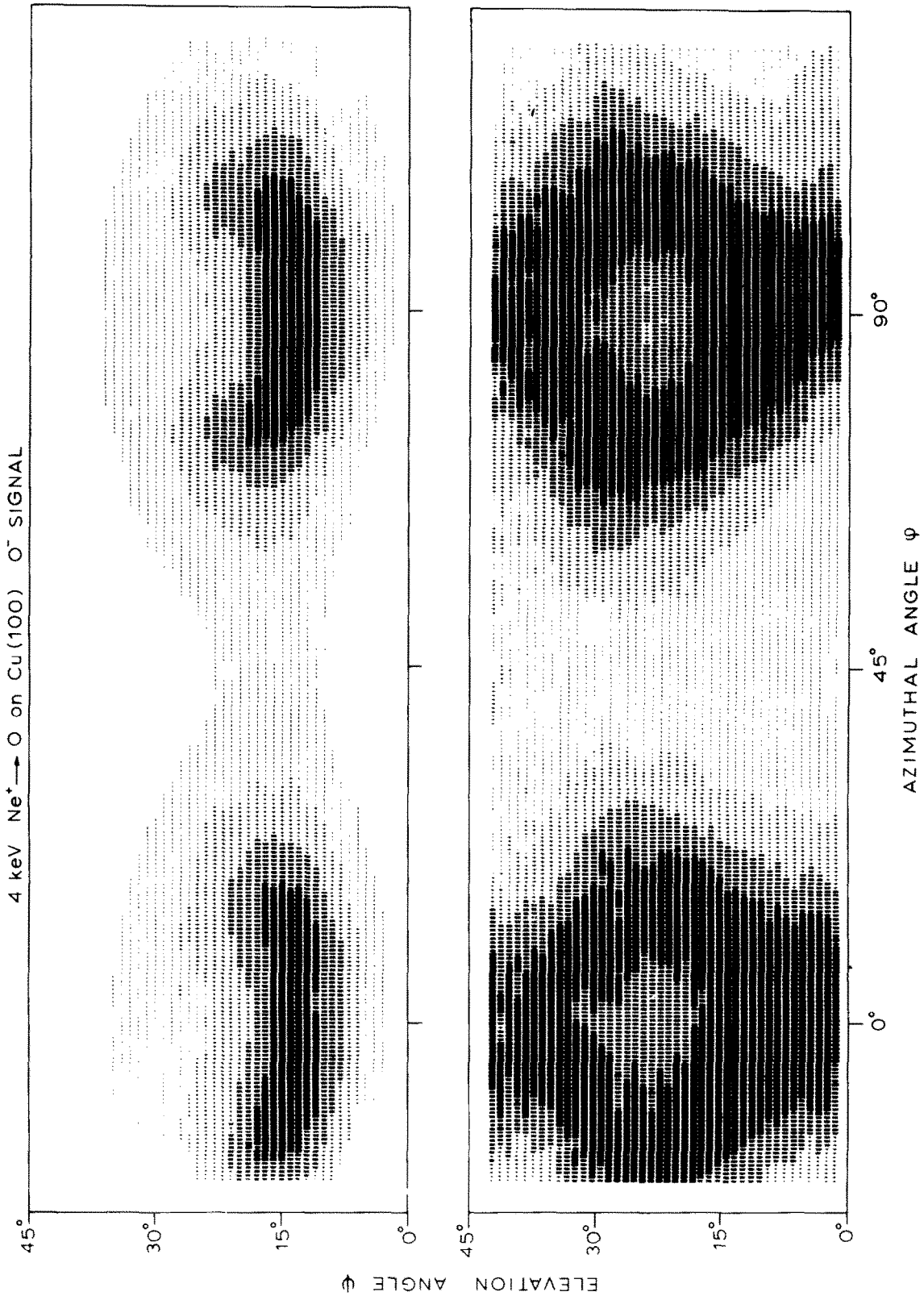


Fig. 4. Photograms for an oxygen-covered Cu(100) surface, measured using the O<sup>-</sup> recoil signal. Upper: absolute scaling over the complete photogram. Lower: scaling between zero and maximum intensity per horizontal line.

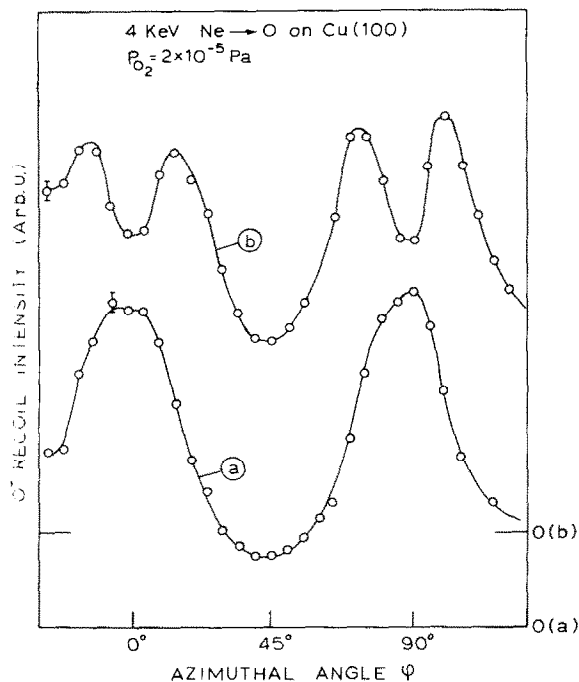


Fig. 5. Azimuthal distribution of  $O^-$  recoil ions. The curves (a) and (b) are plotted to scale: a)  $\psi = 7^\circ$ , b)  $\psi = 24^\circ$ .

only part of the atoms may take place, leading to shallower shadow dips. If oxygen is adsorbed at equivalent sites at the surface, which are not equivalent to the incoming beam direction (for instance the [011] bridge position), shadowing of only part of the oxygen atoms will take place.

It is clear that if reconstruction of the surface takes place or if oxygen atoms are adsorbed at essentially different sites, the interpretation of the angular distributions becomes very problematical.

Nevertheless it appears possible to draw a number of conclusions from the azimuthal distributions of  $O^-$  recoils, if it is assumed that the oxygen-covered Cu surface is not reconstructed (or only by small displacements of the copper atoms). The justification for this assumption will be given in sect. 5.

From the large shallow shadow zones around  $\phi = 45^\circ$ , centred around  $\psi \leq 0^\circ$ , it can be concluded that part of the oxygen atoms are adsorbed at the four-fold hollow site near the surface level. The high background intensity of  $O^-$  recoil ions in this zone, together with the lack of sharp shadow zones at suitable incidence directions make an accurate determination of this oxygen position impossible. This four-fold site must be located at approximately the height of the first copper surface layer, which is in agreement with the oxygen position as proposed by Onuferko and Woodruff [16] and Godfrey

and Woodruff [17]. The fact that a substantial number of oxygen atoms is still visible in the large shadowing and blocking area around  $\phi = 45^\circ$  already is an indication that more oxygen atoms are adsorbed at essentially different sites.

The shadow dip that is observed in the  $O^-$  recoil photograph (fig. 4) at  $\phi = 0^\circ$ ,  $\psi = 22^\circ$  can be explained either by shadowing by oxygen at a location above the surface of the oxygen atoms at the fourfold hollow site or by shadowing by copper atoms of oxygen at a site beneath the  $\langle 110 \rangle$  surface strings. The site above the surface appears to be the most likely one, because there is no shadowing observed in other incidence directions and because of the relative high  $O^-$  recoil intensity that is observed at small elevation angles of incidence. If we assume that the oxygen is indeed adsorbed above the surface, then the site proposed by Onuferko and Woodruff [16] and Godfrey and Woodruff [17] seems to be the most likely possibility: the two-fold bridge site at approximately  $1.4 \text{ \AA}$  above the first copper surface layer. The shadow dip at  $\phi = 0^\circ$ ,  $\psi = 22^\circ$  is then caused by shadowing by oxygen at the two-fold site of oxygen that is located at the fourfold site at a lateral distance of  $3/2 \times 2.56 \text{ \AA}$ .

The dip at  $\phi = 0^\circ$ ,  $\psi = 22^\circ$  became less pronounced for larger exposures. Although this may in principle be explained by a changing electron attachment probability for various incidence angles with coverage, it can much more simply be explained by a changing ratio of the coverages  $\theta_1$  and  $\theta_2$  for the respective sites. In a subsequent paper we shall report the results of an exploratory study on the variation of  $\theta_1$  and  $\theta_2$  with exposure [28].

## 5. The characteristics of the first two copper atom layers

Definite conclusions regarding any possible oxygen position can only be drawn if the geometry of the oxygen-covered Cu{100} surface is known. In order to determine any possible changes in the location of the copper atoms, we studied several polar and azimuthal distributions of the Ne|Cu reflection yield, for a clean and oxygen-covered copper surface. An overall picture of these surfaces is presented in the photograph of fig. 6.

A set of typical azimuthal distributions is given in fig. 7 (The intensities for clean and oxygen-covered copper are not to scale.) The adsorption of oxygen resulted in the following changes in the angular distributions:

- an overall decreasing intensity by about a factor of two,
- a larger decrease of the intensity for directions where deeper layers are visible,
- a small increase of the intensity in the shadowing dips for the main crystallographic surface directions.

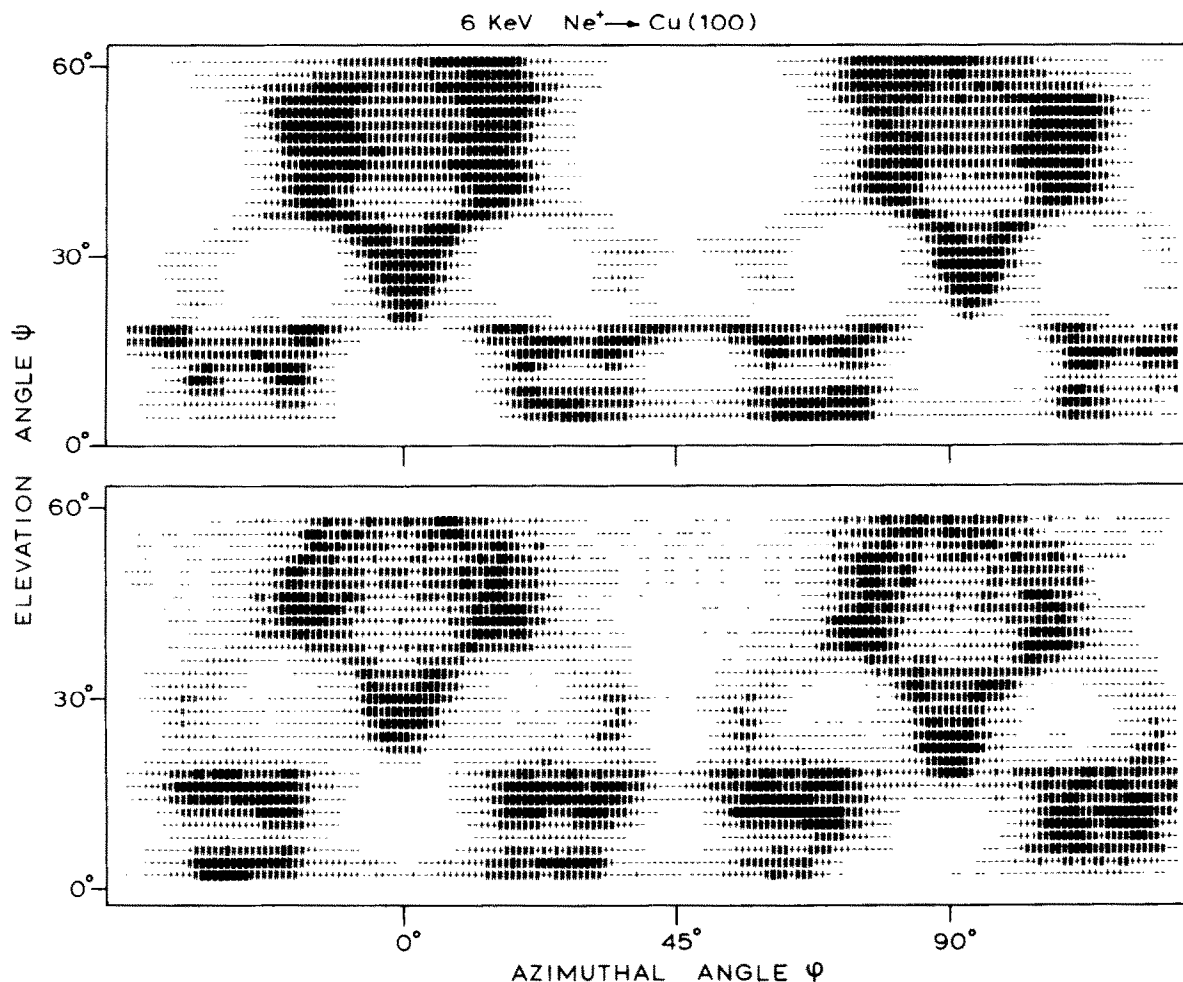


Fig. 6. Upper: photogram of a clean Cu(100) surface (Ne<sup>+</sup> | Cu reflection yield). Lower: photogram of an oxygen-covered Cu(100) surface ( $P_{O_2} = 8 \times 10^{-4}$  Pa).

The decreasing intensity can be explained as usual, by the increasing neutralization probability due to the presence of oxygen at the surface. (In preliminary measurements using reflected neutrals, which were not energy-analyzed, practically no differences were observed between angular distributions of the clean and oxygen-covered Cu{100} surface.) Although the structure in the azimuthal distributions for the oxygen-covered surface became less pronounced, due to the effects mentioned above, the width and position of all shadow dips remained practically unaltered. This strongly suggests that the oxygen-covered Cu{100} surface (stage B) is *not* reconstructed. However, from the increased intensity in the shadow zones it can be concluded that some of the copper atoms are less neatly arranged at the surface. We have measured a similar effect on the other low index copper surfaces; the most pronounced increase of the “background” intensity was found for the oxygen-covered Cu{111} surface, both when using Ne<sup>+</sup> and O<sup>-</sup>

backscattered particles. Niehus [29] observed an increased intensity in the shadow zones of He<sup>+</sup>, backscattered from oxygen-covered Cu{111}, whereas a decreasing intensity was observed for random incidence directions. It seems unlikely that the observed surface roughening of these oxygen-covered copper surfaces is caused by ion-beam induced damage, because the surface roughening is also “visible” after low ion doses at small angles of incidence. (If the mobility of copper atoms is reduced in the vicinity of oxygen atoms, the thermal annealing of damage sites would become less effective.)

It should be noted that the angular distributions are always measured in a dynamical situation: the actual oxygen coverage is determined by the oxygen flow and the number of desorbing oxygen atoms. If the adsorption or incorporation process is governed by a mechanism in which the copper atoms are temporarily removed to a somewhat higher position (see e.g. refs. [3,9]) this might result in an average number of displaced

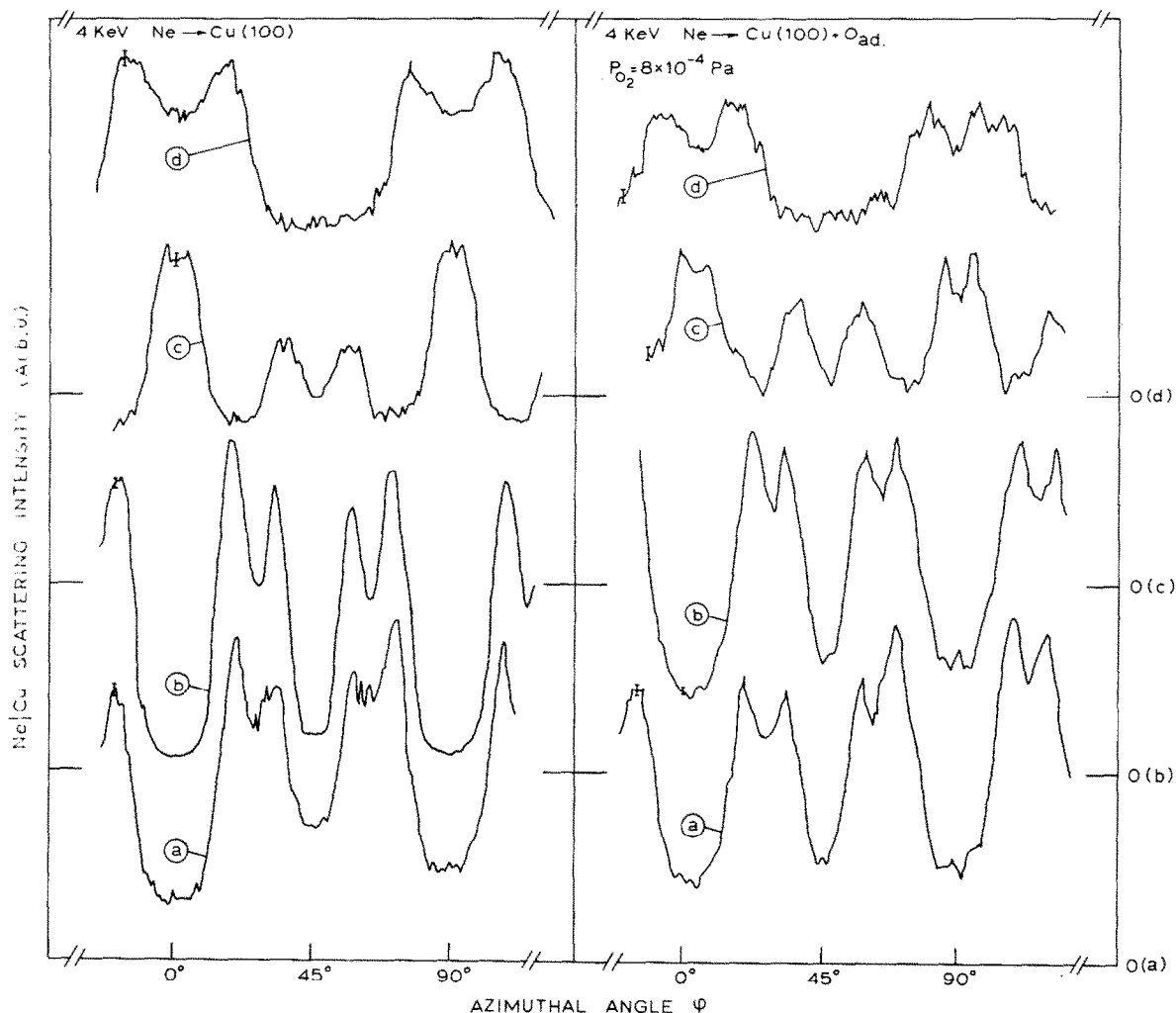


Fig. 7. Set of azimuthal distributions of the  $\text{Ne}^+ | \text{Cu}$  reflection intensity, for a clean and oxygen-covered Cu(100) surface; (a)  $\psi = 9^\circ$ , (b)  $\psi = 13^\circ$ , (c)  $\psi = 31^\circ$ , (d)  $\psi = 53^\circ$ .

copper atoms, depending on the partial oxygen pressure and on the ion beam intensity.

## 6. Conclusion

On the basis of angular distributions of  $\text{O}^-$  recoil ions, we concluded that at least two essentially different oxygen sites are involved at stage B. These sites may well be the sites as proposed by Onuferko and Woodruff: the 2-fold bridge site 1.4 Å above the copper surface and the 4-fold hollow site at approximately the height of the first copper layer. The oxygen-covered Cu(100) (at stage B) surface is not reconstructed, except for a certain surface roughening.

It is very difficult to obtain more information on the basis of azimuthal distributions, because of the four-fold

symmetry of the surface. More information on the adsorption process can be obtained by studying the kinetics of the  $\text{O}_2/\text{Cu}(100)$  system while using signals with a different sensitivity for oxygen at different locations. The results of an exploratory study by our group in this field will be published in a subsequent paper.

This work is part of the research program of the Stichting voor Fundamenteel Onderzoek der Materie (FOM) and was made possible by financial support from the Nederlandse Organisatie voor Zuiver Wetenschappelijk Onderzoek (ZWO).

## References

- [1] R.N. Lee and H.L. Farnsworth. *Surface Sci.* 3 (1965) 461.
- [2] G. Ertl. *Surface Sci.* 6 (1967) 208.

- [3] G.W. Simmons, D.F. Mitchell and K.R. Lawless, *Surface Sci.* 8 (1967) 130.
- [4] T.A. Delchar, *Surface Sci.* 27 (1971) 11.
- [5] L. McDonnell and D.P. Woodruff, *Surface Sci.* 46 (1974) 505.
- [6] L. McDonnell, D.P. Woodruff and K.A.R. Mitchell, *Surface Sci.* 45 (1975) 1.
- [7] D.R. Lloyd, C.M. Quinn and N.V. Richardson, *Surface Sci.* 68 (1977) 419.
- [8] J.R. Noonan, D.M. Zehner and L.H. Jenkins, *Surface Sci.* 69 (1977) 731.
- [9] P. Hofmann, R. Unwin, W. Wyrobisch and A.M. Bradshaw, *Surface Sci.* 72 (1978) 635.
- [10] C. Benndorf, B. Egert, G. Keller and F. Thieme, *Surface Sci.* 74 (1978) 216.  
C. Benndorf, B. Eggert, G. Keller, H. Seidel and F. Thieme, *J. Phys. Chem. Solids* 40 (1979) 877.
- [11] S.P. Holland, B.J. Garrison and N. Winograd, *Phys. Rev. Lett.* 43 (1979) 220.
- [12] C.S. Fadley, S. Kono, L.G. Petersson, S.M. Goldberg, N.F.T. Hall, J.T. Lloyd and Z. Hussain, *Surface Sci.* 89 (1979) 52.  
S. Kono, C.S. Fadley, N.F.T. Hall and Z. Hussain, *Phys. Rev. Lett.* 41 (1978) 117.
- [13] a) F.H.P.M. Habraken, Thesis, University of Utrecht (1980).  
b) F.H.P.M. Habraken, C.M.A.M. Mesters and G.A. Bootsma, *Surface Sci.* 97 (1980) 264.
- [14] P.J. Jennings and G.L. Price, *Surface Sci.* 95 (1980) L205.
- [15] D.T. Ling, J.N. Miller, D.L. Weissman, P. Pianetta, P.M. Stefan, I. Linday and W.E. Spicer, *Surface Sci.* 95 (1980) 89.
- [16] J.H. Onuferko and D.P. Woodruff, *Surface Sci.* 95 (1980) 555.
- [17] D.J. Godfrey and D.P. Woodruff, *Surface Sci.* 105 (1981) 459.
- [18] A. Oustry, L. Lafourcade and A. Escaut, *Surface Sci.* 40 (1973) 545.
- [19] A.G.J. de Wit, Thesis, University of Utrecht (1979).
- [20] A.G.J. de Wit, R.P.N. Bronckers, Th.M. Hupkens and J.M. Fluit, *Surface Sci.* 90 (1979) 676.
- [21] R.P.N. Bronckers, Thesis, University of Utrecht (1981).
- [22] R.P.N. Bronckers and A.G.J. de Wit, *Surface Sci.* 112 (1981) 133.
- [23] R.P.N. Bronckers, Th.M. Hupkens, A.G.J. de Wit and W.C.N. Post, *Nucl. Instr. and Meth.* 179 (1981) 125.
- [24] Th.M. Hupkens and J.M. van Zoest, *Nucl. Instr. and Meth.* B6 (1985) 538.
- [25] Th.M. Hupkens, Thesis, University of Utrecht (1983).
- [26] A. van Veen, Thesis, University of Utrecht (1979).
- [27] A. van Veen, A.G.J. de Wit, G.A. van de Schootbrugge and J.M. Fluit, *J. Phys. E* 12 (1979) 861.
- [28] Th.M. Hupkens, *Nucl. Instr. and Meth.*, following paper, this issue, *Nucl. Instr. and Meth.* B9 (1985) 285.
- [29] H. Niehus, *Surface Sci.* 130 (1983) 41.
- [30] C.B. Duke, N.O. Lipari and G.E. Laramore, *Il Nuovo Cimento* 23B (1974) 241.